AD

TECHNICAL REPORT ARCCB-TR-99005

A PROGRESS REPORT ON X-RAY DIFFRACTION MEASUREMENTS ON NEW LOW-THERMAL CONDUCTIVITY THERMOELECTRIC MATERIALS

ANNE P. HYNES
SABRINA L. LEE
SANDRA B. SCHUJMAN
GLEN A. SLACK

APRIL 1999

US ARMY ARMAMENT RESEARCH,
DEVELOPMENT AND ENGINEERING CENTER
CLOSE COMBAT ARMAMENTS CENTER
BENÉT LABORATORIES
WATERVLIET, N.Y. 12189-4050

DISCLAIMER

The findings in this report are not to be construed as an official Department of the Army position unless so designated by other authorized documents.

The use of trade name(s) and/or manufacturer(s) does not constitute an official endorsement or approval.

DESTRUCTION NOTICE

For classified documents, follow the procedures in DoD 5200.22-M, Industrial Security Manual, Section II-19, or DoD 5200.1-R, Information Security Program Regulation, Chapter IX.

For unclassified, limited documents, destroy by any method that will prevent disclosure of contents or reconstruction of the document.

For unclassified, unlimited documents, destroy when the report is no longer needed. Do not return it to the originator.

REPORT DOCUMENTATION PAGE

Form Approved
OMB No. 0704-0188

1. AGENCY USE ONLY *(Leave blank)*	2. REPORT DATE	3. REPORT TYPE AND DATES COVERED
	April 1999	Final

4. TITLE AND SUBTITLE

A PROFRESS REPORT ON X-RAY DIFFRACTION MEASUREMENTS ON NEW LOW-THERMAL CONDUCTIVITY THERMOELECTRIC MATERIALS

5. FUNDING NUMBERS

AMCMS No. 6111.01.91A1.1

6. AUTHOR(S)

Anne P. Hynes (RPI, Troy, NY), Sabrina L. Lee,
Sandra B. Schujman (RPI), and Glen A. Slack (RPI)

7. PERFORMING ORGANIZATION NAME(S) AND ADDRESS(ES)

U.S. Army ARDEC
Benet Laboratories, AMSTA-AR-CCB-O
Watervliet, NY 12189-4050

8. PERFORMING ORGANIZATION REPORT NUMBER

ARCCB-TR-99005

9. SPONSORING/MONITORING AGENCY NAME(S) AND ADDRESS(ES)

U.S. Army ARDEC
Close Combat Armaments Center
Picatinny Arsenal, NJ 07806-5000

10. SPONSORING/MONITORING AGENCY REPORT NUMBER

11. SUPPLEMENTARY NOTES

12a. DISTRIBUTION/AVAILABILITY STATEMENT

Approved for public release; distribution unlimited.

12b. DISTRIBUTION CODE

13. ABSTRACT *(Maximum 200 words)*

Thermoelectric devices and materials have potential applications in refrigeration and power generation. An X-ray diffraction study was made documenting the phase and the lattice parameter of both some new thermoelectric compounds and some previously known compositions. The materials contained primarily Ir, Rh, Sb, Sn, and Pt. Improvements in the measurement procedures resulted in improved accuracy in lattice parameter measurements and in peak intensity measurements.

14. SUBJECT TERMS

Thermoelectric Materials, Ir, Rh, Sb, Sn, Pt,
Skutterud, Lattice Parameters

15. NUMBER OF PAGES

21

16. PRICE CODE

17. SECURITY CLASSIFICATION OF REPORT	18. SECURITY CLASSIFICATION OF THIS PAGE	19. SECURITY CLASSIFICATION OF ABSTRACT	20. LIMITATION OF ABSTRACT
UNCLASSIFIED	UNCLASSIFIED	UNCLASSIFIED	UL

TABLE OF CONTENTS

TABLES

LIST OF ILLUSTRATIONS

ACKNOWLEDGEMENTS

The authors gratefully acknowledge support from ONR Contract No. N00014-94-1-0341 and the Watervliet Benet Laboratories.

INTRODUCTION

A semiconductor thermoelectric device comprises two different semiconductors that are electrically joined at both ends. When the junctions are maintained at two different temperatures, an electromotive force proportional to the temperature difference is established (ref 1). Alternately, when two semiconductors are joined and maintained at a constant temperature while a current passes through the junction, heat (in addition to the joule heat) is generated or absorbed at the junction. These devices have found applications in refrigeration and power generation for space satellites (refs 2, 3). While thermoelectrics has been studied for more than 175 years, most of the work conducted during the past 30 years has focused on optimizing the properties of compounds such as those based on Bi_2Te_3 and Bi-Sb, Si-Ge and PbTe (ref 2). Recently, there has been an increased interest in using thermoelectrics for refrigeration applications for which the presently used vapor-compression method is unsuitable—such as cooling microelectronics or laser diodes (ref 3). Conventional refrigerators evaporate and condense a fluid (e.g., chlorofluorocarbon) that absorbs heat when the fluid boils and releases heat to the outside when the fluid cools. Thermoelectrics perform the same function—with electrons as the only moving parts and no environmentally unfriendly gases. Thermoelectric generators can also improve fuel efficiency by using the heat lost from an automobile engine, presently about two-thirds of an engine's power, to run an electric power generator (ref 3).

One new material with promising thermoelectric properties is the skutterudite system, which is found in Skutterud, Norway. Skutterudite consists of $CoAs_3$, which is cubic. Other metals in this family include Ir, Co, or Rh combined with P, As, or Sb. They have a clathrate structure (ref 4) that contains "cages" of atoms into which impurity atoms or dopants can be inserted. A desirable thermoelectric conducts electrons as well as metal and conducts heat as poorly as glass (ref 5). A number of new materials with a clathrate structure have been fabricated at the Novel Materials Laboratory at Rensselaer (ref 6), and this progress report summarizes the results of X-ray diffraction analyses of some of these materials, specifically $IrSb_3$, $RhSb_3$, $RhSb_3$ with Bi and/or Sn, $PtSb_2Sn$ and Sr-Sn clathrates.

One of the authors prepared the powders by reaction of the required stoichiometric elemental powders at temperatures 300^0C under argon; details of the procedures have been reported previously (refs 6-8). After reaction, the powders were ground using a mortar and pestle, and milled with tungsten carbide balls to prepare powder samples for X-ray diffraction.

EXPERIMENTAL PROCEDURE

X-ray Diffraction Equipment

The X-ray diffraction measurements were performed on a SCINTAG XDS 3000 diffractometer in the Bragg-Brentano geometry. The diffractometer used a long, fine-focus Cu tube operated at 1800 watts (45kV - 40mA), which yields a wavelength of Cu-$K_{\alpha 1}$ of 1.5406Å. The XDS 3000 was equipped with a Peltier-cooled Si-Li-drifted detector and 2- and 4-mm soller slits in the incident and diffracted beams. A monochromator was not used. Receiving slits of 0.2

and 0.5 mm were used for the first scans; receiving slits of 0.1 and 0.3 mm were used for later scans. No filters were used. The incident beam slits were not theta-compensating. The takeoff angle was 6 degrees.

Types of Scans

Scans were made with two goals in mind—to determine phase analysis and lattice parameter—which usually required two different scans. For phase analysis, a relatively fast scan was made from 10-100° (2θ) using a step size of 0.02-0.05°and a hold time (preset time) of 1-2s. For lattice parameter measurement, all scans were done in a step-scan mode, from 10-130° (2θ) using a step size of 0.02° and a hold time (preset time) of 5s. Initially, the scans were conducted overnight; to avoid running overnight, later scans were made in two segments, from 10 to 60 or 65° and from 60 or 65°to 130°.

The X-ray tube was warmed up with the one-day, two-day or one-week program before each run, as appropriate.

The sample preparation and measurement procedures have undergone some development and exploration, which are still in progress. Initial samples were not ground as finely as recent samples, which have been ball-milled to a particle size of <10 μm. The initial scans, which were in a continuous mode and/or with relatively large (>0.02°) step sizes, were quickly found to yield insufficient accuracy; therefore, smaller step sizes and longer count times were used for the step scan. Initial lattice parameter measurements were made on a glass slide with a National Institute of Science and Technology (NIST) (formerly NBS, the National Bureau of Standards) internal standard of Si, SRM640b. This standard permits correcting the angular position for inherent instrument bias and sample height, but is not a standard for intensity. The difference between the measured and certified angular positions for each Si peak was fitted to a polynomial that was then used to correct the peak positions for the sample. The lattice parameter was found by least-squares fitting the calculated lattice parameter for each peak against the Nelson-Riley function $[(\cos^2\theta/\sin\theta) + (\cos^2\theta/\theta)]$ and extrapolating the best-fit line back to $2\theta = 90°$, where the errors are minimized. Although this procedure has been used for many years to measure lattice parameters and is sufficient for lattice parameter measurements to ~0.01Å or better, its accuracy and precision were insufficient for the estimated measurement of 0.0001Å.

For these lattice parameter determinations, the diffractometer was aligned before measurements were taken, and the calibration was checked with NIST standard material SRM1976—a sintered corundum (α-Al_2O_3) plate, 3-cm square—before each set of consecutive runs. This standard covers the angular range of the samples of interest. For each calibration run, $\Delta(2\theta)$ versus (2θ) was plotted to examine the error in 2θ, where $\Delta(2\theta) = 2\theta_{SRM} - 2\theta_{obs}$. Another plot was made of the intensity ratio $[I_{obs}/I_{SRM}]$ versus 2θ. Figure 1 shows an example of calibration plots. The target error in 2θ was $|0.01°|$, with as high as $|0.02°|$ acceptable; the target for the intensity ratio was |0.612| , with as much as |0.650| acceptable.

Sample Preparation

Phase analysis samples were loaded by sprinkling the powder on double-stick tape mounted on a glass slide (or subsequently, a quartz plate). No internal standard was used for the phase analysis runs. To minimize the preferred orientation effects, some tests were conducted to side-load the samples for structure determination using a small holder of cut glass slides; however, an insufficient amount of the sample adhered to the tape. Consequently, samples were back-loaded or sprinkled onto a low-background holder with a piece of double-stick tape. The low-background holder consists of a quartz crystal slice cut such that no significant diffraction peaks are present. This holder lowers background noise considerably. Future tests may be run with a holder that contains a sample "well," or indentation, to increase the volume of diffracted material and thus increase the measured peak intensity. The method has not been used before because it requires a greater amount of sample and probably a binder, which can add spurious lines to the diffractogram.

For the lattice parameter runs, two scans were made for each composition: one with an internal standard to correct lattice position and intensity; these data were used to calculate lattice parameter. The other, without the internal standard, will be used for Rietveld structure refinement. The internal standard currently used is SRM676, which is a fine, plasma-sprayed, α-Al_2O_3 powder. The particles do not exhibit the preferred orientation, and SRM676 is the only available certified intensity standard. This material has peaks that cover the angular range of the samples of interest, although NIST has not certified the intensities for the entire range. Unlike the Si SRM640b standard, the α-Al_2O_3 SRM676 standard covers the lower angles of the compounds of interest. While the SRM676 peak positions are not certified, they can be accurately calculated from the certified values of the lattice parameters. The standard and sample are well-mixed in acetone with a porcelain mortar and pestle to attain 2θ without the standard.

Data Analysis

For phase analysis, the background was subtracted and $K_{\alpha 2}$ was removed from the raw data using the SCINTAG software package *Background Subtraction*. A user-defined Periodic Table that contained only those elements used to prepare the sample helped to narrow the search field of possible phases found by the *Search/Match* program. The stick patterns of the matches and the sample were compared to determine the phases present. In some cases, the tabulated peak positions were used also.

The peak position for the lattice parameter measurement is determined from a fit of the raw data using the SCINTAG-DMS software program *Profile-fit* and a split-Pearson function with a fixed ratio $[K_{\alpha 1}/K_{\alpha 2}]$. The $\Delta(2\theta)$ versus 2θ for the internal standard is plotted and fit to a polynomial, which is then used to correct the peak positions of the sample. A similar procedure is used with the intensity ratio to correct sample intensities. Since the certified data for internal standard SRM676 were derived in the theta-compensating geometry, the SRM intensity values must first be multiplied by the factor $(1/\sin\theta)$ for comparison with this work.

Measuring line intensities is more difficult than measuring d-spacings/lattice parameter, and a consensus has not been reached regarding the procedures. The most significant open areas of discussion include: the role of Rietveld analysis (whether it should be used as an adjunct to the X-ray data analysis or whether it is as important as the diffraction measurements (ref 9); the actual intensity values of the corundum standards (which seem to depend on the details of the slit arrangement of each piece of equipment) (ref 10); and the number of measurements required to precisely measure intensity, including how to minimize preferred orientation (refs 9-11).

RESULTS AND DISCUSSION

$IrSb_3$

The nominal $IrSb_3$ powder was single-phase $IrSb_3$, and the lines matched powder diffraction file (PDF) card No. 17-888. The lattice parameter was calculated with a Nelson-Riley analysis and used an Si standard. The lattice parameter was 9.2501Å, which agrees (within experimental error) with the card value of 9.2495 Å and the value of 9.2503Å obtained by Slack and Tsoukala (ref 12). Figure 2 depicts a plot of the data.

To determine whether Ar could be included in the structure, $IrSb_3$ powders were treated twice with a hot-isostatic-press (HIP) using Ar gas, and with an HIP of the $IrSb_3$ powder using Ar and BN powder. After the HIP, both samples contained the $IrSb_3$, and the sample with BN exhibited the presence of BN, as expected. The lattice parameter of the three samples agreed within the range of experimental error; therefore, as Ar did not increase the lattice parameter significantly, little if any Ar entered the samples. This interpretation is supported by previously reported mass spectroscopy results (refs 6, 7). While these analyses found no Ar in the $IrSb_3$ - BN mixtures, Ar was present in a sample without BN that was heated with Ar under a pressure of 27 kpsi at 1000°C for 100h, implying that some of the Ar was trapped within the voids of the clathrate during sintering (refs 6-8).

$RhSb_3$

The $RhSb_3$ powder comprised primarily the compound $RhSb_3$, which agreed with microprobe results (refs 6-8). The diffraction pattern agreed with PDF card no. 19-1041 for $RhSb_3$—with the exception of the six lines shown in Table 1. These lines could not be attributed to Rh, Sb, or any Rh-Sb compound in the PDF. The lattice parameter, which was measured similarly for $IrSb_3$, had a value of 9.22980.0013Å, which agrees with the PDF card value of 9.229Å. The best literature value, 9.23220.0006Å, from Kjekshus and Rakke (ref 13) is slightly larger. Figure 3 is a plot of the data.

Table 1. Unidentified Diffraction Peaks in Nominal $RhSb_3$ Powder

d (Å)	I_{rel} (%)
5.33	22.00
4.59	25.00
2.31	5.00
1.78	5.00
1.25	10.00
1.06	4.00

$RhSb_3$ with Bi and/or Sn

Three rhodium triantimonide compositions with Bi and one without were analyzed for phase composition. The nominal compositions of the powders are shown in Table 2. Bi was added in an attempt to incorporate Bi atoms into the voids in the crystal structure, and Sn was added in some cases to provide charge balance for the suspected Bi^{3+} ions (ref 7) (see Figure 4).

Table 2. Nominal Compositions of $RhSb_3$ with Bi and/or Sn

Nominal Composition	Maximum Fraction of Voids Filled (%)	Charge Compensation
$Rh_{40}Sb_{120}Bi$	10	No
$Rh_8Sb_{21}Sn_3Bi$	50	Yes
$Rh_4Sb_9Sn_3Bi$	100	Yes
$Rh_4Sb_{12}Sn_2$	0	NA

Nominal composition $Rh_{40}Sb_{120}Bi$ displayed a diffraction pattern that closely matched PDF card no. 19-1041 for $RhSb_3$, and this was interpreted as evidence of the presence of a skutterudite. Microprobe analysis confirmed the presence of $RhSb_3$ with no Bi in the skutterudite phase and also found a secondary phase with the approximate composition of $Sb_{0.9}Bi_{0.1}$ (refs 6-8).

Nominal composition $Rh_8Sb_{21}Sn_3Bi$ also showed a diffraction pattern that closely matched PDF card no. 19-1041 for $RhSb_3$, which again was interpreted to indicate the presence of a skutterudite. Only two low-intensity peaks were unaccounted for by the skutterudite: 3.090Å, with I_{rel} = 11% and 3.171Å, with I_{rel} = 5%. An analysis using a microprobe confirmed the presence of a phase with the composition Rh_4Sb_{12} Sn_1 that was similar to that of PDF card no. 19-1041 for $RhSb_3$, and this was presumed to be a skutterudite phase. Small spots of a Bi second phase and a phase with composition $RhSb_2$ $Sn_{0.1}$ were also found (refs 6-8).

Nominal composition $Rh_4Sb_9Sn_3Bi$ also exhibited a diffraction pattern that closely matched PDF card no. 19-1041 for $RhSb_3$, indicating the presence of a skutterudite structure. In addition, the nominal composition contained a small amount of SbBi (PDF card no. 35-0517). Five additional lines were present, most of which were consistent with small amounts of elemental Sb (PDF card no. 35-0712) and SbSn (PDF card no. 01-0830).

When the as-prepared powder of nominal composition $Rh_4Sb_{12}Sn_2$ was analyzed for phase composition, all of the peaks except one (~1.766Å and I_{rel} ~4%) could be attributed to skutterudite PDF card no.19-1041 for $RhSb_3$. Two peaks that did not match the card at ~3.044Å and I_{rel} ~16% and ~2.782Å and I_{rel} ~3% could be attributed to two lines that were not allowed by the space group for the reflections [300] and [311]. A very small amount of elemental Sn (PDF card no. 04-0673 or 05-0390) may be present; however, Sn cannot be positively identified due to a possible overlap with the lines of the $RhSb_3$ phase.

The conclusion, based on these X-ray results combined with the electron-beam microprobe results, is that no Bi enters the voids in the skutterudite structure of $RhSb_3$. These results are similar to the Bi-$IrSb_3$ (ref 14) and Bi-$CoSb_3$ (ref 15) phase studies, which showed that no Bi was incorporated. Thus, the fraction of the voids actually filled in Table 2 is zero, not 10, 50 or 100 percent.

$PtSb_2Sn$

Four samples of nominal composition $PtSb_2Sn$ were analyzed for phase composition—the as-prepared powder and the powder after hot-pressing at three conditions (500°C for 2h, 600°C for 1h, and 1050°C for 0.5h). Figure 5 displays the data.

The as-prepared powder exhibited a pattern that was very close to PDF card no. 19-1041 for $RhSb_3$, and this is interpreted as indicating a skutterudite phase. The diffractogram also contained approximately 21 "extra" peaks, which did not index to the skutterudite phase; approximately half could be indexed by relaxing the diffraction restriction (h+k+l=2n). The remaining peaks did not match the known powder diffraction file of elemental compounds, binaries, or ternaries of Pt-Sb-Sn; they may represent a new phase. The unindexed peaks are listed in Table 3. The lattice parameter, as determined with a Nelson-Riley analysis and an Si standard, was 9.2250.087Å.

Table 3. Unidentified Diffraction Lines of Nominal $PtSb_2Sn$ As-Prepared at 700°C for 75h (2x) (refs 6-8)

d (Å)	I_{rel} (%)
3.81	8.00
3.30	17.00
3.18	33.00
2.86	30.00
2.199	9.00
2.174	7.00
2.088	76.00
1.990	9.00
1.913	22.00
1.906	40.00
1.830	30.00
1.476	7.00

The diffraction results for the powder that was hot-pressed at 500°C for 2h showed a skutterudite (presumably equivalent to $PtSb_3$), and microprobe results also detected a phase close to this composition, i.e., $PtSb_{1.9}Sn_{1.1}$ (ref 8). Also present in the diffraction pattern were lines for a phase similar to $PtSb_{1.3}Sn$ (PDF card no. 22-0784). A match was also found with cubic phase $PtSn_2$ (PDF card no. 07-0371), but since microprobe analysis found small regions of composition $PtSb_{1.9}Sn_{0.1}$ and the nominal powder composition was closer to $PtSb_2$, a similar structure may have resulted from the substitution of Sb on Sn sites.

The powder that was hot-pressed at 600°C for 1h contained the skutterudite (also found in microprobe $PtSb_{1.8}Sn_{1.3}$ [ref 8]), plus a phase similar to $PtSb_{1.3}Sn$, PDF card no. 22-0784 (microprobe found $PtSb_{1.5}Sn_{0.5}$ [ref 8]), as well as $PtSb_2$, PDF card no. 14-0141 (microprobe found $PtSb_{1.8}Sn_{0.2}$ [ref 8]). If either elemental Sn (PDF card no. 04-0673) or $PtSn_2$ (PDF card no. 07-0371) is present, it is overlapped by other lines. Pt_2Si (PDF card no. 17-0683) accounts for most of the remaining lines; however, since no Si was included in the powder preparation, perhaps a compound with a similar structure is present. The lines that remain after these phases are subtracted are shown in Table 4.

The powder that was hot-pressed at 1050°C for 0.5h evidently contained a skutterudite phase since the pattern was similar to PDF card no. 19-1041 for $RhSb_3$. In addition, it contained SbSn (either PDF card no. 01-830 or PDF card no. 33-118) and a phase similar to $PtSb_{1.3}Sn$ (PDF card no. 22-0784). Microprobe analysis found phases that were similar in composition to the three ($PtSb_{1.8}Sn_{1.3}$, $PtSb_{1.8}Sn_{0.2}$, and $PtSb_{1.5}Sn_{0.5}$, respectively) as well as an Sn phase that contained a small amount of Sb ($Sn_{0.9}Sb_{0.1}$) (refs 6-8).

Table 4. Unidentified Diffraction Lines of Nominal $PtSb_2Sn$ After Hot-Pressing at 600°C for 1h (refs 6-8)

d (Å)	I_{rel} (%)
7.16	18.00
4.13	35.00
2.28	43.00
1.61	12.00
1.428	9.00
1.414	5.00
1.045	8.00

Sr-Sn Clathrates

Two compositions of Sr-Sn clathrates (nominal compositions $Sr_8In_{16}Sn_{30}$ and $Sr_8Ga_{16}Sn_{30}$) supplied by George Nolas were quickly scanned for phase composition. (The preparation conditions and further analyses will be described elsewhere [ref 16]). The diffraction patterns for the samples were compared with known phases that contained the given elements and other phases that closely matched. Figures 6 and 7 display the data. The phases that are listed in the powder diffraction file or otherwise known and that contain only elements Sr, In, and Sn or Sr, Ga, and Sn are presented in Tables 5a, 5b, and 6.

Table 5a. Phases in the Powder Diffraction File Containing Only Sr, Ga, and Sn

Composition	Phase	PDF Card No.
Sr + Ga + Sn	None	--
Sr + Sn	SrSn	23-0553
	SrSn	41-1314
	Sr_2Sn	31-1364
	Sr_2Sn	32-1265
Sr + Ga	Ga_4Sr	18-0543
	GaSr*	32-0402
Ga + Sn	None	--

*New data show no such compound at atmospheric pressure.

Table 5b. Phases Reported in Literature Containing Only Sr, Ga, and Sn

Composition	Phase	Reference
Sr + Sn	Sn_3Sr	17
	Sn_4Sr	
	Sn_5Sr	
Sr + Ga	Ga_2Sr	18
	Ga_2Sr_3	19

Table 6. Phases in the Powder Diffraction File Containing Only Sr, In, and Sn

Composition	Phase	PDF Card No.
In + Ga + Sn	None	--
In + Ga	$Ga_{0.84}In_{0.16}$	33-0556
	$Ga_{0.9}In_{0.1}$	34-1437
Ga + Sn	None	--
In + Sn	In_3Sn	07-0345
	$InSn_4$	07-0396

Powder with the nominal composition $Sr_8In_{16}Sn_{30}$ matched the patterns of $InSn_4$ (PDF card no. 07-0396). Only two lines with relative intensities greater than 5 percent were unaccounted for by this phase, and these occurred at 2.911Å and I_{rel} = 7% and 2.715Å and I_{rel} = 18%.

The powder with the nominal composition $Sr_8Ga_{16}Sn_{30}$—which was heat-treated (CL02)—contained lines of Sn (PDF card no. 04-0673) and other lines that matched the structure of Pt_3Si (PDF card no. 43-1133). Powder with the same nominal composition of $Sr_8Ga_{16}Sn_{30}$, but which was heat-treated at (CL03), matched the pattern of Sn (PDF card no. 04-0673) and Pt_3Si (PDF card no. 43-1133) as well. Both phases contained lines that did not match any other known phases. These lines were at 3.116Å and 100%; 1.637Å and 27%; 1.357 and 1.243Å, both 8%; 1.109Å and 82%; and 1.045Å and 5%. The Pt_3Si phase matches were unexpected (10 of 11 lines match, the eleventh line is of low intensity) since no source of Pt or Si was identified in the procedure; however, the matches were so close that a compound with a similar structure and lattice parameter is likely to be present. Phase Pt_3Si (PDF card no. 43-1133) is cubic, space group Pm3m (221), with a lattice parameter of 3.88Å. There is no Sr_3Sn and no Ga_3Sn phase listed in the powder diffraction file. However, phase In_3Sn (PDF card no. 07-0345) is tetragonal with a = 4.89Å (very close to c = 4.45Å and nearly cubic), so an unidentified Ga_3Sn phase may exist.

REFERENCES

1. *American Institute of Physics Handbook*, 2nd ed., D.E. Gray, editor, McGraw-Hill Book Co., New York, 1963, pp. 9-33.

2. Nolas, G.S., Slack, G.A., Morelli, D.T., Tritt, T.M., and Erlich, A.C., "The Effect of Rare-Earth Filling on the Lattice Thermal Conductivity of Skutterudites," *Journal of Applied Physics*, **79**[8] (1996) 4002.

3. Wu, C., "A Silent Cool: Thermoelectrics May Offer New Ways to Refrigerate and Generate Power," *Science News*, **152** (1997) 152-153.

4. Pauling, L. and Marsh, R.E., "The Structure of Chlorine Hydrate," *Proceedings of the National Academy of Sciences*, **38** (1952) 112-118.

5. Slack, G.A., personal communication, Rensselaer Polytechnic Institute, Troy, N.Y., 1997.

6. Slack, G.A., Schujman, S.B., and Hynes, A.P., "New Low-Thermal Conductivity Thermoelectric Materials," presented at ONR Solid State and Material Chemistry Review meeting, Alexandria, Va., October 6-8, 1997.

7. Slack, G.A., FY97 End of Fiscal Year letter, ONR Contract: Thermoelectric Materials Research for Naval Application for Contract No. N00014-94-1-0341, September 1997.

8. Schujman, S.B., "Novel Materials Laboratory," a seminar for the Physics, Applied Physics and Astronomy Departments, Rensselaer Polytechnic Institute, Troy, N.Y., 1997.

9. Cline, J., personal communication, National Institute of Standards and Technology, 1997.

10. Robie, S., personal communication, Scintag, Inc., 1997.

11. Wong-Ng, W. and Hubbard, C., personal communication, National Institute of Standards and Technology, 1997.

12. Slack, G. and Tsoukala, V., "Some Properties of Semiconducting $IrSb_3$," *Journal of Applied Physics*, **76[3]** (1994) 1665-1671.

13. Kjekshus, A. and Rakke, T., *Acta Chemica Scandinavica*, **28A** (1974) 99-103.

14. Slack, G. A. and Nolas, G., unpublished data, Rensselaer Polytechnic Institute, Troy, N.Y., 1996.

15. Dudkin, L.D. and Abrikosov, N. Kh, "On the Doping of the Semiconductor Compound $CoSb_3$," *Soviet Physics–Solid State*, **1** (1959) 126-133.

16. Nolas, G., et al., in preparation, Rensselaer Polytechnic Institute, Troy, N.Y.

17. Widera, A. and Schafer, H., "Das Zustandsdiagramm Sr-Sn und Die Verbindung Sr_3SnO," *The Journal of the Less Common Metals*, **77** (1981) 29-36.

18. Iandelli, A., "Crystallographic Studies of the Systems M Al_2-M Ga_2 (M=Yb, Ca, Eu, Sr)," *The Journal of the Less Common Metals*, **135** (1987) 195-198.

19. Bruzzone, G., "I Sistemi Binary Ca-Ga, Sr-Ga, Ba-Ga," *Bollettino Scientifico dell Facolta di Chimica Industriale di Bologna*, **24[4]** (1966) 113-132.

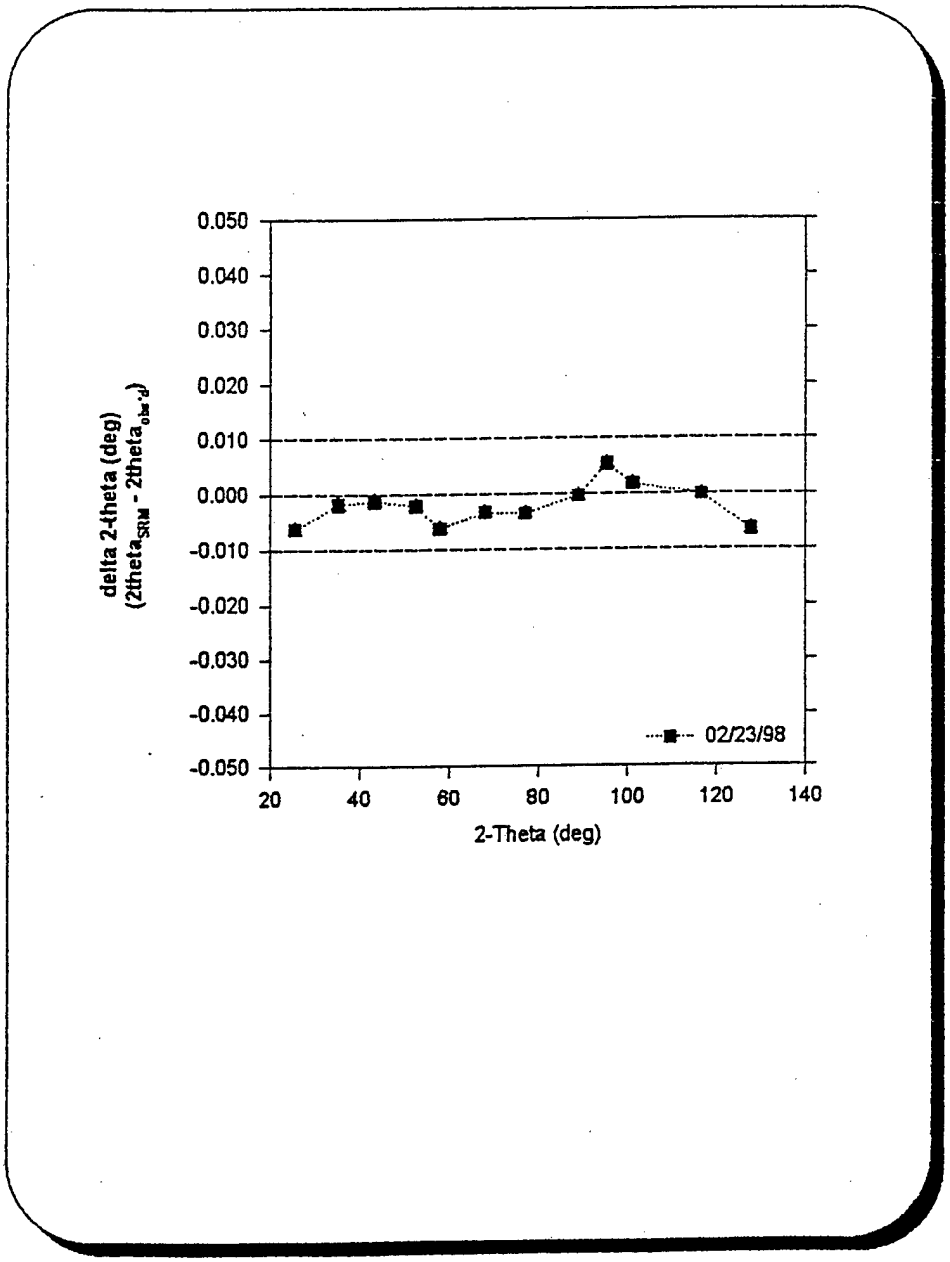

Figure 1. Calibration plot for SRM1976 standard Delta-2Theta vs. 2Theta.

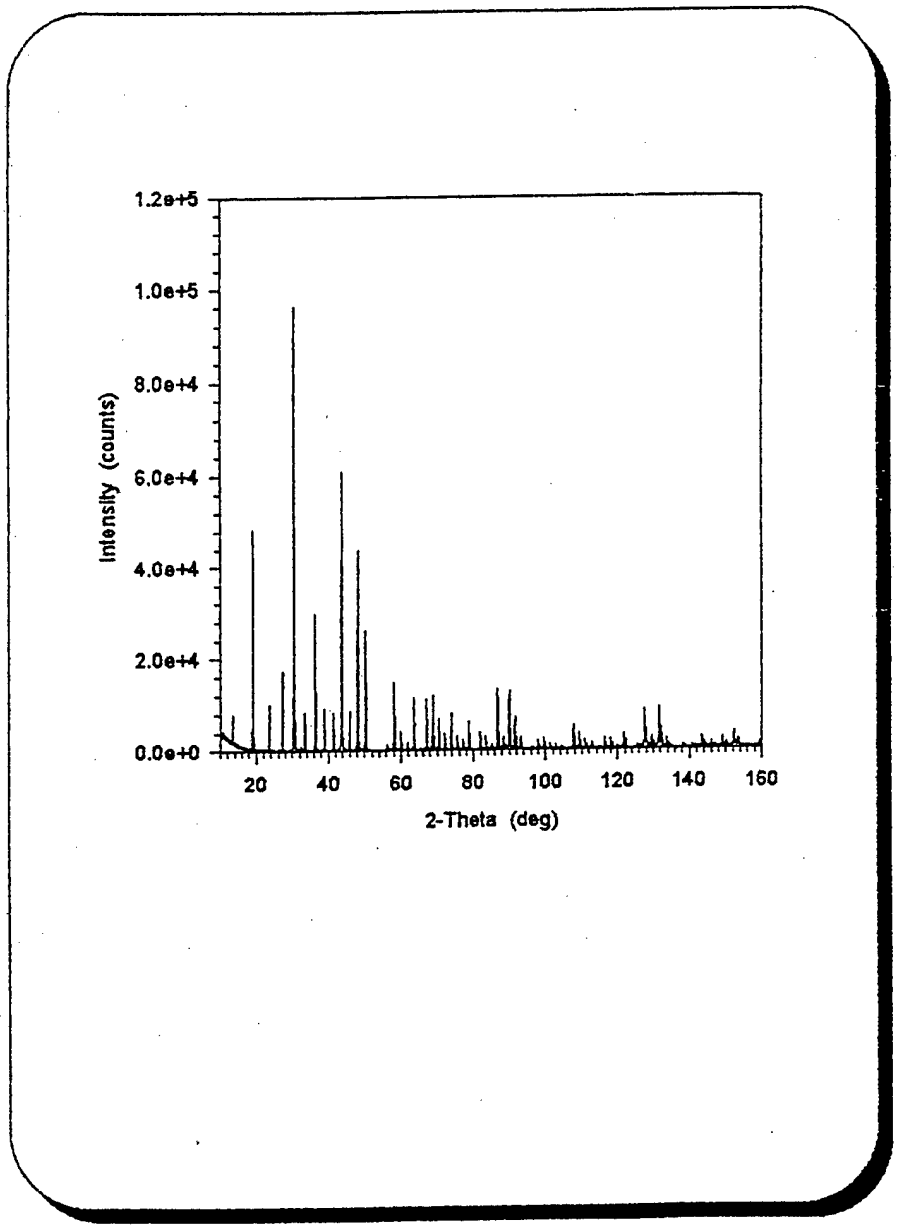

Figure 2. X-ray diffraction pattern of $IrSb_3$ using copper radiation.

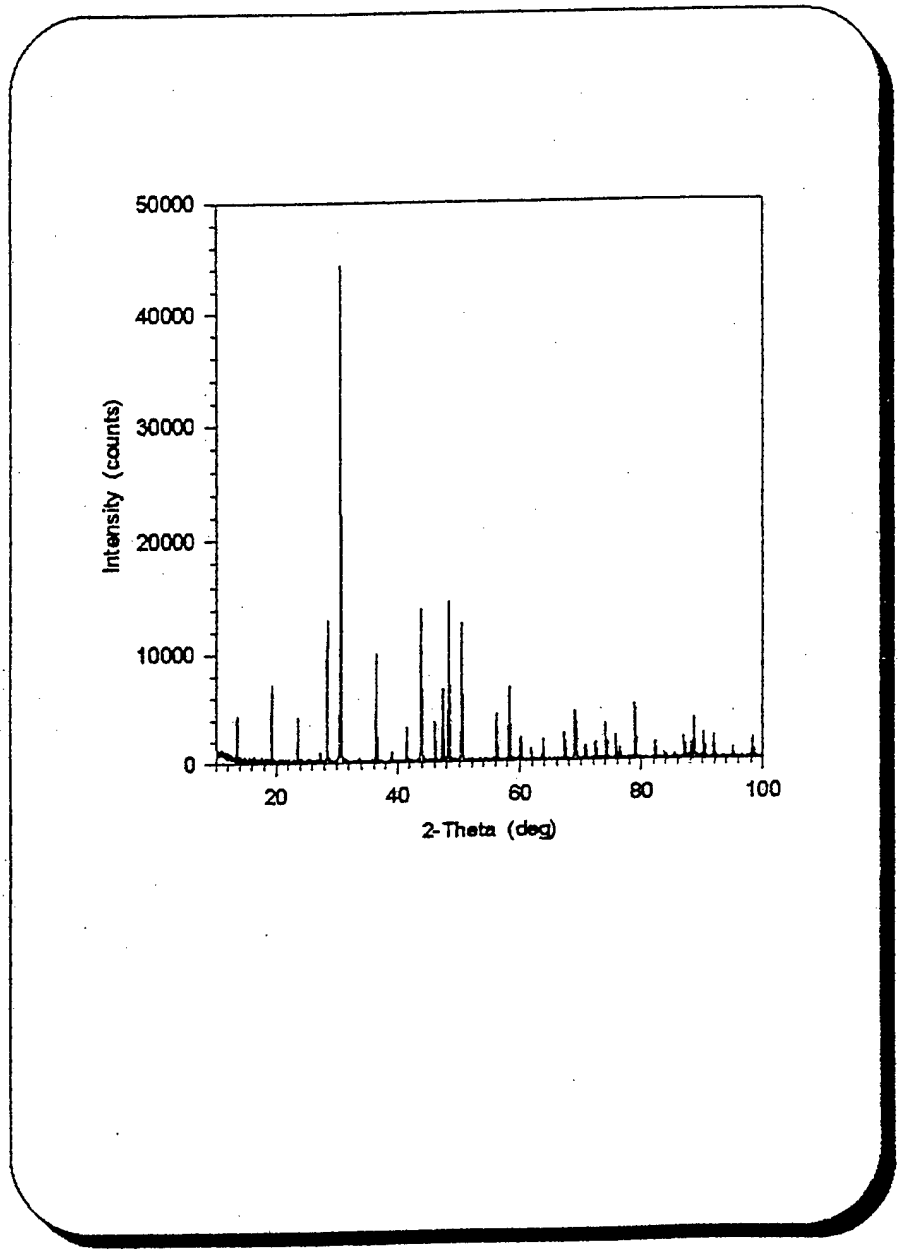

Figure 3. X-ray diffraction pattern of $RhSb_3$ using copper radiation.

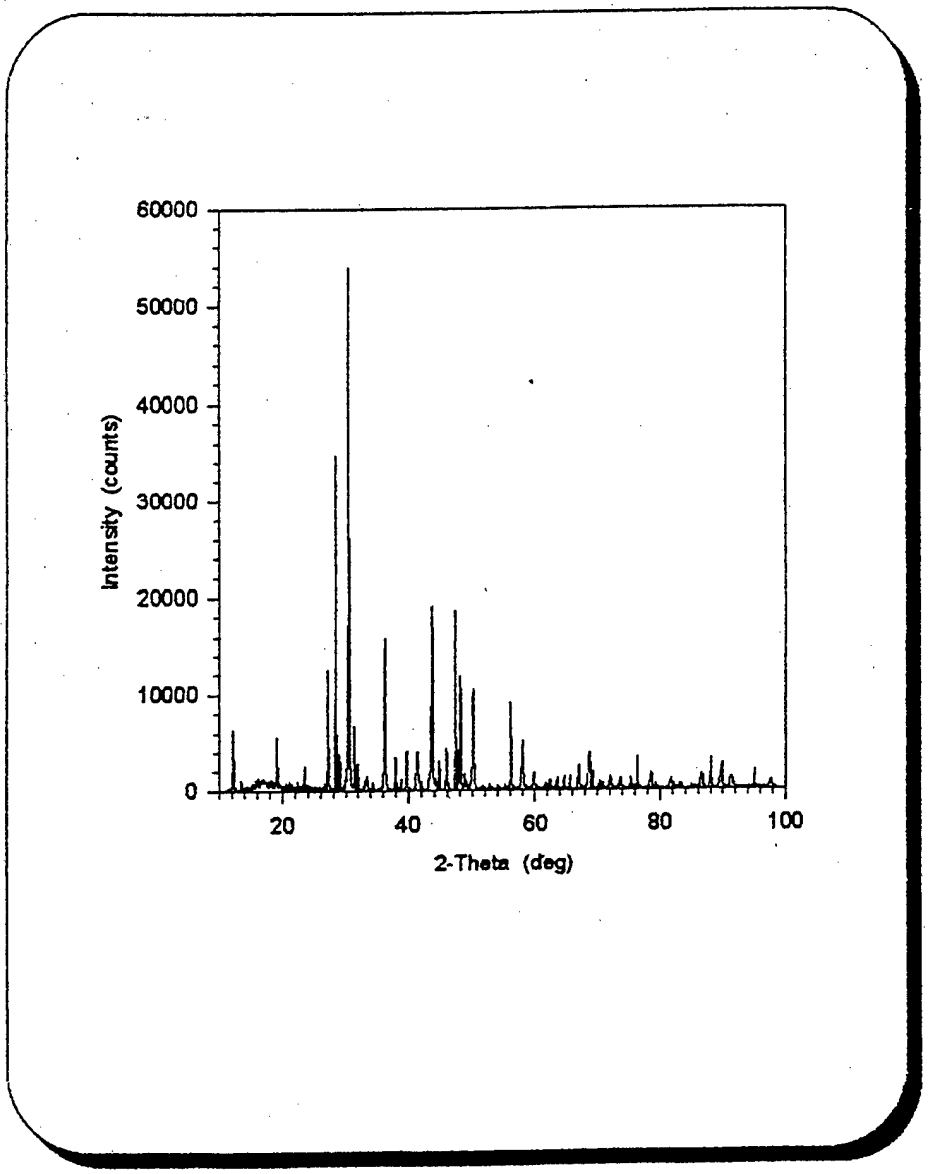

Figure 4. X-ray diffraction pattern of $Rh_4Sb_9Sn_3Bi$ using copper radiation.

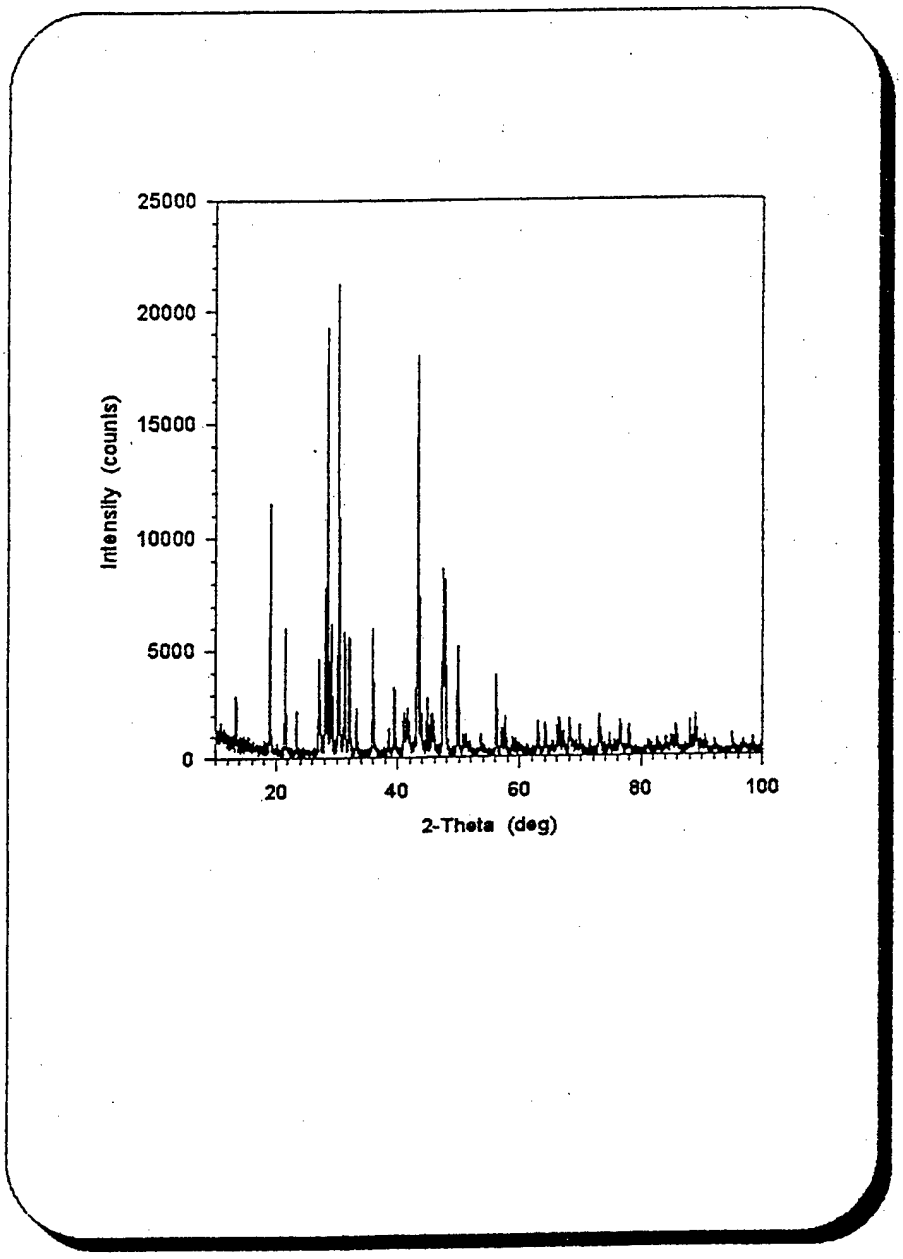

Figure 5. X-ray diffraction pattern of $PtSb_2Sn$ using copper radiation.

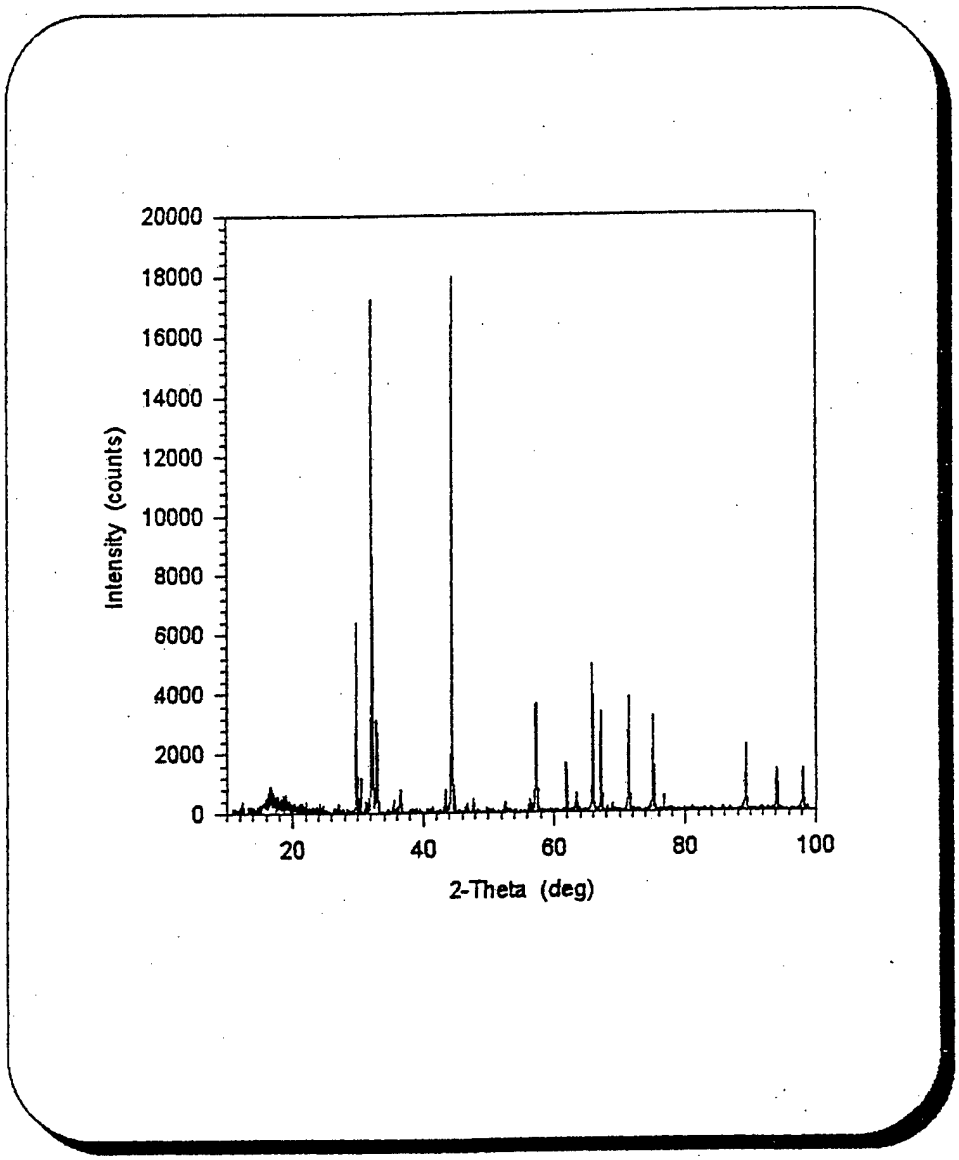

Figure 6. X-ray diffraction pattern of $Sr_8In_{16}Sn_{30}$ using copper radiation.

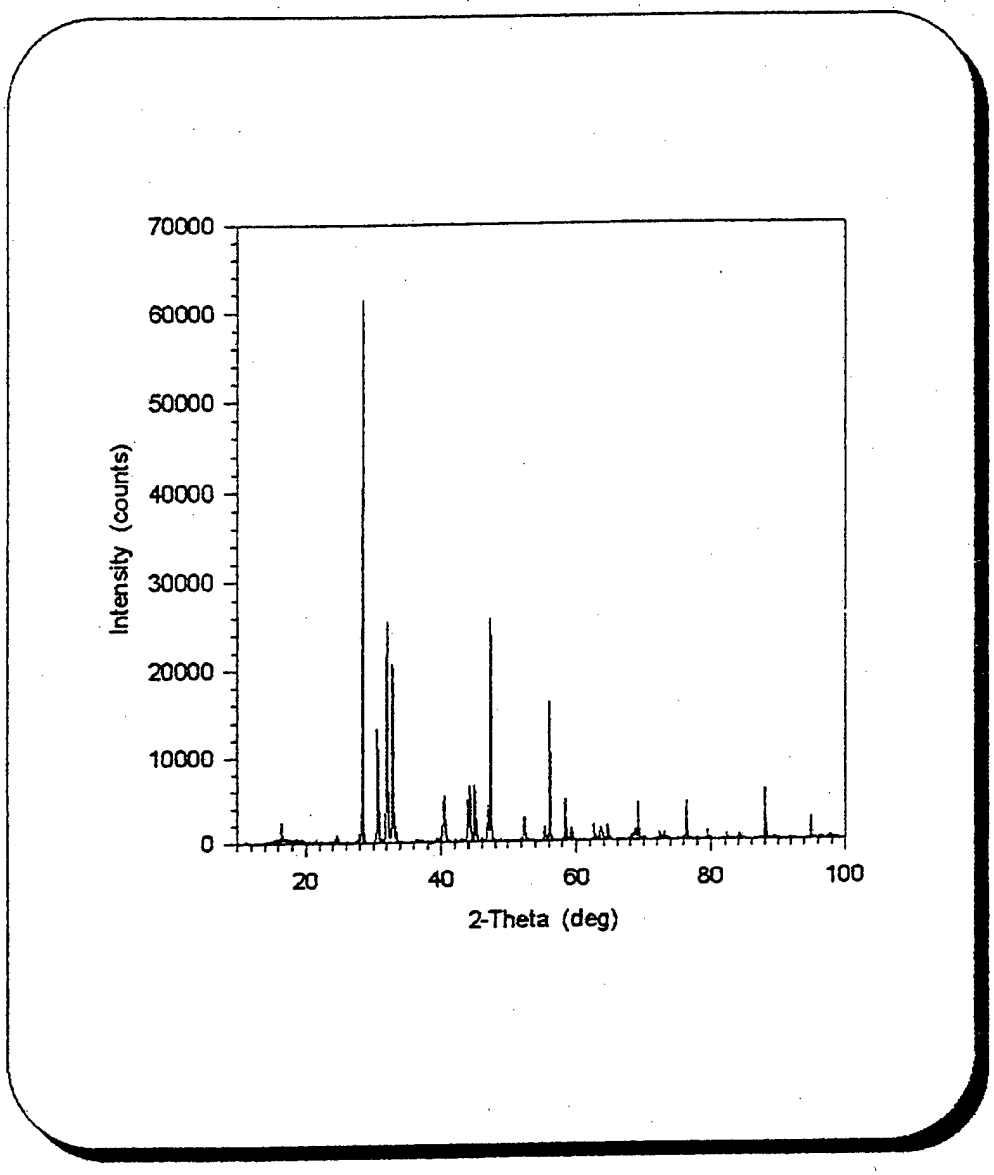

Figure 7. X-ray diffraction pattern of $Sr_8Ga_{16}Sn_{30}$ using copper radiation.

TECHNICAL REPORT INTERNAL DISTRIBUTION LIST

	NO. OF COPIES
CHIEF, DEVELOPMENT ENGINEERING DIVISION	
ATTN: AMSTA-AR-CCB-DA	1
-DB	1
-DC	1
-DD	1
-DE	1
CHIEF, ENGINEERING DIVISION	
ATTN: AMSTA-AR-CCB-E	1
-EA	1
-EB	1
-EC	1
CHIEF, TECHNOLOGY DIVISION	
ATTN: AMSTA-AR-CCB-T	2
-TA	1
-TB	1
-TC	1
TECHNICAL LIBRARY	
ATTN: AMSTA-AR-CCB-O	5
TECHNICAL PUBLICATIONS & EDITING SECTION	
ATTN: AMSTA-AR-CCB-O	3
OPERATIONS DIRECTORATE	
ATTN: SIOWV-ODP-P	1
DIRECTOR, PROCUREMENT & CONTRACTING DIRECTORATE	
ATTN: SIOWV-PP	1
DIRECTOR, PRODUCT ASSURANCE & TEST DIRECTORATE	
ATTN: SIOWV-QA	1

NOTE: PLEASE NOTIFY DIRECTOR, BENÉT LABORATORIES, ATTN: AMSTA-AR-CCB-O OF ADDRESS CHANGES.

TECHNICAL REPORT EXTERNAL DISTRIBUTION LIST

	NO. OF COPIES
DEFENSE TECHNICAL INFO CENTER ATTN: DTIC-OCA (ACQUISITIONS) 8725 JOHN J. KINGMAN ROAD STE 0944 FT. BELVOIR, VA 22060-6218	2
COMMANDER U.S. ARMY ARDEC ATTN: AMSTA-AR-WEE, BLDG. 3022 AMSTA-AR-AET-O, BLDG. 183 AMSTA-AR-FSA, BLDG. 61 AMSTA-AR-FSX AMSTA-AR-FSA-M, BLDG. 61 SO AMSTA-AR-WEL-TL, BLDG. 59 PICATINNY ARSENAL, NJ 07806-5000	 1 1 1 1 1 2
DIRECTOR U.S. ARMY RESEARCH LABORATORY ATTN: AMSRL-DD-T, BLDG. 305 ABERDEEN PROVING GROUND, MD 21005-5066	 1
DIRECTOR U.S. ARMY RESEARCH LABORATORY ATTN: AMSRL-WM-MB (DR. B. BURNS) ABERDEEN PROVING GROUND, MD 21005-5066	 1
COMMANDER U.S. ARMY RESEARCH OFFICE ATTN: TECHNICAL LIBRARIAN P.O. BOX 12211 4300 S. MIAMI BOULEVARD RESEARCH TRIANGLE PARK, NC 27709-2211	 1
COMMANDER ROCK ISLAND ARSENAL ATTN: SIORI-SEM-L ROCK ISLAND, IL 61299-5001	 1
COMMANDER U.S. ARMY TANK-AUTMV R&D COMMAND ATTN: AMSTA-DDL (TECH LIBRARY) WARREN, MI 48397-5000	 1
COMMANDER U.S. MILITARY ACADEMY ATTN: DEPT OF CIVIL & MECH ENGR WEST POINT, NY 10966-1792	 1
U.S. ARMY AVIATION AND MISSILE COM REDSTONE SCIENTIFIC INFO CENTER ATTN: AMSAM-RD-OB-R (DOCUMENTS) REDSTONE ARSENAL, AL 35898-5000	 2
COMMANDER U.S. ARMY FOREIGN SCI & TECH CENTER ATTN: DRXST-SD 220 7TH STREET, N.E. CHARLOTTESVILLE, VA 22901	 1

NOTE: PLEASE NOTIFY COMMANDER, ARMAMENT RESEARCH, DEVELOPMENT, AND ENGINEERING CENTER, BENÉT LABORATORIES, CCAC, U.S. ARMY TANK-AUTOMOTIVE AND ARMAMENTS COMMAND, AMSTA-AR-CCB-O, WATERVLIET, NY 12189-4050 OF ADDRESS CHANGES.